## **RSC Advances**



(1)

View Article Online **PAPER** View Journal | View Issue



Cite this: RSC Adv., 2017, 7, 47619

# WO<sub>3</sub>/BiVO<sub>4</sub> photoanode coated with mesoporous Al<sub>2</sub>O<sub>3</sub> layer for oxidative production of hydrogen peroxide from water with high selectivity?

Kojiro Fuku, 📵 \*a Yuta Miyase, ab Yugo Miseki, 📵 a Takahiro Gunji ab and Kazuhiro Sayama\*ab

(eqn (1)).

A WO<sub>3</sub>/BiVO<sub>4</sub> photoanode coated with various metal oxides demonstrated high selectivity (faradaic efficiency) for hydrogen peroxide (H<sub>2</sub>O<sub>2</sub>) generation from water (H<sub>2</sub>O) under irradiation of simulated Received 31st August 2017 solar light in a highly concentrated hydrogen carbonate (KHCO<sub>3</sub>) agueous solution. A mesoporous and amorphous aluminium oxide ( $Al_2O_3$ ) layer significantly facilitated inhibition of the oxidative degradation DOI: 10.1039/c7ra09693c of generated H<sub>2</sub>O<sub>2</sub> into oxygen (O<sub>2</sub>) on the photoanode, resulting in unprecedented H<sub>2</sub>O<sub>2</sub> selectivity (ca. 80%) and the accumulation (>2500  $\mu$ M at 50C).

Accepted 3rd October 2017

rsc.li/rsc-advances

Chemical conversions using light energy have been performed in various fields since the discovery of the Honda-Fujishima effect. 1-25 Significant efforts have recently been devoted to H<sub>2</sub> production by water splitting using inexhaustible light for clean energy conversion processes. 1-4,8-29 Photoelectrode systems are widely recognised as a promising technology for H2 production because they operate at an electrolysis voltage lower than the theoretical electrolysis voltage of water (<1.23 V).<sup>1,8-29</sup> Visible light-responsive oxide photoanodes with a narrow bandgap energy, such as WO<sub>3</sub>, BiVO<sub>4</sub> and Fe<sub>2</sub>O<sub>3</sub>, are desirable for the efficient utilisation of solar light and economical synthetic processes.8-29 Most importantly, numerous efforts have been focused on BiVO<sub>4</sub> photoanodes capable of utilising a wide range of light energy ( $\sim$ 520 nm) and achieving efficient O<sub>2</sub> generation by water splitting.9-21,28,29,32 A WO3/BiVO4 photoanode that combines BiVO<sub>4</sub> with a WO<sub>3</sub> underlayer for the efficient transfer of excited electrons on BiVO<sub>4</sub> to the F-doped SnO<sub>2</sub> conductive glass (FTO) substrate shows exceptional photoelectrochemical performance for water splitting into  $H_2$  and  $O_2$ .  $^{10-13,17-20,28,29,32}$ However, most previous investigations, containing electrochemical reactions, focused solely on the recovery of H<sub>2</sub> energy generated on the cathode and little attention was paid to the recovery of the oxidation products simultaneously evolved during water splitting.24-31

Recently, we reported that a photoelectrochemical system combining the WO<sub>3</sub>/BiVO<sub>4</sub> photoanode and aqueous electrolyte of KHCO3 under CO2 bubbling could achieve simultaneous generation and accumulation of H2O2 and H2 from H2O (eqn (3)). 28,29 In this system, the aqueous electrolyte of KHCO3 acts as an excellent oxidative catalyst for generating H<sub>2</sub>O<sub>2</sub> from H<sub>2</sub>O. Moreover, H<sub>2</sub>O<sub>2</sub> could be produced at no external bias on both a WO<sub>3</sub>/BiVO<sub>4</sub> photoanode (from H<sub>2</sub>O) and an Au cathode (from  $O_2$ ) via a two-photon process (eqn (4)).<sup>29</sup>

 $H_2O_2$  is an especially versatile and clean oxidation product

However, the accumulation of H<sub>2</sub>O<sub>2</sub>, generated oxidatively is

extremely difficult because degradation of H2O2 into O2 also

occurs easily and oxidatively in a conventional photo-

electrochemical system i.e. the redox potential of H<sub>2</sub>O<sub>2</sub> degra-

dation is more negative than the redox potential of H2O2

production from H<sub>2</sub>O (eqn (1) and (2)), resulting in low selec-

having the potential to generate instead of O2 from H2O

 $2H_2O \rightarrow H_2O_2 + 2H^+ + 2e^- (E(H_2O_2/H_2O) =$ 

+1.77 V vs. RHE)

tivity for oxidative H2O2 generation.

$$2H_2O \rightarrow H_2O_2 + H_2$$
 (two-photon process) (3)

$$2H_2O + O_2 \rightarrow 2H_2O_2$$
 (two-photon process) (4)

Although the selectivity (faradaic efficiency:  $\eta(H_2O_2)$ ) of reductive H<sub>2</sub>O<sub>2</sub> production from O<sub>2</sub> on cathodes such as Au was very high, almost 100%, the maximum selectivity  $(\eta(H_2O_2))$  for oxidative H<sub>2</sub>O<sub>2</sub> production on WO<sub>3</sub>/BiVO<sub>4</sub> photoanodes was still

 $H_2O_2 \rightarrow O_2 + 2H^+ + 2e^- (E(O_2/H_2O_2) = +0.68 \text{ V } vs. \text{ RHE})$  (2)

<sup>&</sup>lt;sup>a</sup>Research Center for Photovoltaics (RCPV), National Institute of Advanced Industrial Science and Technology (AIST), Central 5, 1-1-1 Higashi, Tsukuba, Ibaraki 305-8565, Japan. E-mail: k.sayama@aist.go.jp

<sup>&</sup>lt;sup>b</sup>Department of Pure and Applied Chemistry, Tokyo University of Science, 2641 Yamasaki, Noda, Chiba 278-8514, Japan

<sup>†</sup> Electronic supplementary information (ESI) available: Experimental section, SEM images, XRD spectra, LHE spectra, applied voltage properties, I-V characteristic of photoanodes, pore size distribution of the  $MeO_x$  particles, effect of Al<sub>2</sub>O<sub>3</sub> amount on WO<sub>3</sub>/BiVO<sub>4</sub> and dependence of applied voltage. See DOI: 10.1039/c7ra09693c

**RSC Advances** Paper

low, only ca. 54%. The design of novel photoanodes capable of achieving efficient H<sub>2</sub>O<sub>2</sub> generation and inhibiting oxidative degradation of generated H2O2 is absolutely imperative for building a clean and breakthrough technology, by accumulating H<sub>2</sub>O<sub>2</sub> and H<sub>2</sub> with unprecedented H<sub>2</sub>O<sub>2</sub> selectivity using only H<sub>2</sub>O as the raw material.

Here, we focused on a surface modification of the metal oxide (MeO<sub>r</sub>) layers on the WO<sub>3</sub>/BiVO<sub>4</sub> photoanode surface to achieve excellent selectivity of generation and accumulation of H<sub>2</sub>O<sub>2</sub> in the KHCO<sub>3</sub> aqueous solution under simulated solar light irradiation (Fig. 1). The MeO<sub>x</sub> layers were prepared by spincoating of metal organic solutions and calcination. Introducing a porous Al<sub>2</sub>O<sub>3</sub> layer was found to specifically permit oxidative H<sub>2</sub>O<sub>2</sub> generation and accumulation with exceptional selectivity in an aqueous KHCO<sub>3</sub> electrolyte because of the blocking effect of oxidative degradation of the generated H2O2 into O2 on the photoanode.

Details regarding experimental procedures for preparation and photoelectrochemical reactions of photoanodes are provided in the ESI†.

The effects of MeOx layers, modified on the WO3/BiVO4 photoanode, for oxidative H2O2 generation properties were investigated at an applied electric charge of 0.9C (900 s at steady photocurrent of 1 mA) in a 0.5 M KHCO<sub>3</sub> aqueous electrolyte. As shown in Fig. 2, all MeO<sub>x</sub>-coated photoanodes, except CoO<sub>x</sub>, enhanced the oxidative H2O2 generation compared to a bare WO<sub>3</sub>/BiVO<sub>4</sub> photoanode, and the enhanced effect, ranked by the modified metal oxide, was  $Al_2O_3 > ZrO_2 > TiO_2 > SiO_2 >> CoO_r$ . Little  $H_2O_2$  was observed on the  $CoO_x$  coated photoanode, because CoO<sub>x</sub> probably decomposed the generated H<sub>2</sub>O<sub>2</sub> quickly, or  $O_2$  may be evolved on  $CoO_x$  directly. It should be noted that the Al<sub>2</sub>O<sub>3</sub> modification on the WO<sub>3</sub>/BiVO<sub>4</sub> photoanode achieved roughly twice the oxidative H<sub>2</sub>O<sub>2</sub> generation compared to the bare WO<sub>3</sub>/BiVO<sub>4</sub> photoanode. The Al<sub>2</sub>O<sub>3</sub> uniformly, smoothly and flatly covered the entire area of the WO<sub>3</sub>/BiVO<sub>4</sub> photoanode as shown in the SEM images (Fig. 3), whereas other MeO<sub>x</sub> were granularly and uniformly supported on that and possessed any crack holes (Fig. S1; ESI†). It was also confirmed, from XRD measurement (Fig. S2; ESI†), that no

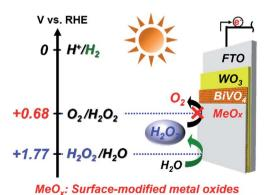


Fig. 1 Pattern and energy diagrams for photoelectrochemical H<sub>2</sub>O<sub>2</sub> generation from H<sub>2</sub>O on WO<sub>3</sub>/BiVO<sub>4</sub>/MeO<sub>x</sub> photoanodes under solar light irradiation.

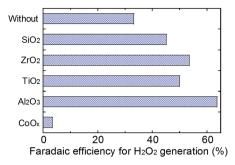


Fig. 2 Oxidative H<sub>2</sub>O<sub>2</sub> generation on photoanodes (WO<sub>3</sub>/BiVO<sub>4</sub>/ MeO<sub>x</sub>) modified various metal oxides on a WO<sub>3</sub>/BiVO<sub>4</sub> at an electric charge of 0.9C (900 s at steady photocurrent of 1 mA) in a 0.5 M KHCO<sub>3</sub> aqueous electrolyte (35 mL) in an ice bath (below 5 °C) under simulated solar light.

diffraction peaks derived from MeO<sub>r</sub> were observed in all WO<sub>3</sub>/ BiVO<sub>4</sub>/MeO<sub>r</sub> photoanodes, suggesting that all tried MeO<sub>r</sub> modified on WO<sub>3</sub>/BiVO<sub>4</sub> photoanode possess amorphous-like structure. As shown in Fig. S3; ESI,† little change of the light harvesting efficiency (LHE) was also confirmed in tried all photoanodes, suggesting that these MeOx introduced on the WO<sub>3</sub>/BiVO<sub>4</sub> have little effect to light absorption efficiency on WO<sub>3</sub>/BiVO<sub>4</sub> photoanode. The time courses of voltages applied between photoanode and a counter electrode of Pt mesh at steady photocurrent of 1 mA (Fig. 2) in oxidative H2O2 generation reaction were also confirmed (Fig. S4; ESI†). The voltages for applying steady photocurrent of 1 mA slightly increased by introducing MeO<sub>x</sub> on the WO<sub>3</sub>/BiVO<sub>4</sub> photoanode. In particular, WO<sub>3</sub>/BiVO<sub>4</sub>/Al<sub>2</sub>O<sub>3</sub> photoanode, coated uniformly, smoothly and flatly at Al<sub>2</sub>O<sub>3</sub> compared to other MeO<sub>x</sub>, required highest applied voltage. In order to confirm the effect introducing the Al<sub>2</sub>O<sub>3</sub> on the photoanode in more detail, the photocurrent property of the WO<sub>3</sub>/BiVO<sub>4</sub>/Al<sub>2</sub>O<sub>3</sub> photoanode was investigated in a 0.5 M KHCO<sub>3</sub> aqueous solution (Fig. S5; ESI†). The bare WO<sub>3</sub>/BiVO<sub>4</sub> photoanode exhibited excellent photocurrent property in all applied voltage ranges as with our past reported example, 11,12,28,29 and the photocurrent property slightly decreased by introducing the Al<sub>2</sub>O<sub>3</sub> layer. However, it should be noted that the decreasing degree of the photocurrent property was slight, only ca. 9% and 5% at +1.23 V and +1.77 V vs. RHE, respectively, although the Al2O3, having an insulation property, covered the entire area of the WO<sub>3</sub>/BiVO<sub>4</sub> photoanode. A similar

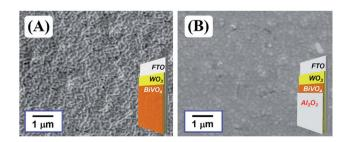


Fig. 3 SEM images of (A) WO<sub>3</sub>/BiVO<sub>4</sub> and (B) WO<sub>3</sub>/BiVO<sub>4</sub>/Al<sub>2</sub>O<sub>3</sub> photoanodes

**Paper** 

phenomenon has also been observed in O2 and H2 generation through water splitting on a photoanode coated with amorphous-like Ta2O5.32 In addition, it was confirmed, from the N<sub>2</sub> absorption and desorption measurement of MeO<sub>x</sub> particles (Fig. S6; ESI $\dagger$ ), that almost all MeO<sub>x</sub> possess mesoporous structure at a pore size of ca. 4-20 nm. In particular, a pore size of the Al<sub>2</sub>O<sub>3</sub> was ca. 4.7 nm. The thicknesses of Al<sub>2</sub>O<sub>3</sub> calculated from the coating amount on the WO<sub>3</sub>/BiVO<sub>4</sub> photoanode by XRF measurement were ca. 100 nm  $(0.055 \text{ mg cm}^{-2})$ . In order to also investigate the effects of dense Al2O3 on WO3/BiVO4 on the oxidative H<sub>2</sub>O<sub>2</sub> generation, increasing Al<sub>2</sub>O<sub>3</sub> amount on WO<sub>3</sub>/ BiVO<sub>4</sub> photoanode was performed by decreasing the spin coating number (500 rpm) of precursor solution of EMOD solved in butyl acetate containing ethylcellulose when introducing Al<sub>2</sub>O<sub>3</sub> layers. The thickness of Al<sub>2</sub>O<sub>3</sub> introduced at 500 rpm calculated from the XRF measurement was ca. 127 nm (0.070 mg cm<sup>-2</sup>), suggested that the thickness increases with decreasing the spin coating number. As shown in Fig. S7; ESI,† little change of the H<sub>2</sub>O<sub>2</sub> generation amounts was observed on these WO<sub>3</sub>/BiVO<sub>4</sub>/Al<sub>2</sub>O<sub>3</sub> photoanodes prepared at 500 and 1000 rpm, indicating that increasing Al<sub>2</sub>O<sub>3</sub> on WO<sub>3</sub>/BiVO<sub>4</sub> photoanode has little effect on the oxidative H<sub>2</sub>O<sub>2</sub> generation. In subsequent experiments, WO<sub>3</sub>/BiVO<sub>4</sub>/Al<sub>2</sub>O<sub>3</sub> prepared at 1000 rpm was utilized as the photoanode. These results indicate that the specific effect enhancing oxidative H<sub>2</sub>O<sub>2</sub> generation property was achieved on the WO<sub>3</sub>/BiVO<sub>4</sub> though the mesoporous and amorphous Al<sub>2</sub>O<sub>3</sub> layer covered uniformly, smoothly and flatly the entire area.

To track the specific performance enhancing effect of generating  $H_2O_2$  by introducing the  $Al_2O_3$  layer, the concentration dependency of KHCO<sub>3</sub> aqueous electrolytes on the oxidative  $H_2O_2$  generation property was investigated at an applied electric charge of 0.9C (Fig. 4(A)). We have already reported that the oxidative  $H_2O_2$  generation property on the WO<sub>3</sub>/BiVO<sub>4</sub> photoanode was improved with increasing concentration of KHCO<sub>3</sub>, which acts as an effective catalyst for  $H_2O_2$ 

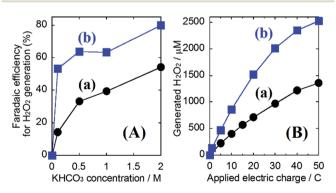


Fig. 4 (A) Oxidative  $H_2O_2$  generation in KHCO $_3$  aqueous electrolytes (35 mL) of different concentrations at applied electric charges of 0.9C (900 s at steady photocurrent of 1 mA) under simulated solar light and (B) accumulation of oxidative  $H_2O_2$  generation in a 2.0 M KHCO $_3$  aqueous solution (35 mL) under visible light irradiation ( $\lambda > 420$  nm) using an intense Xe lamp at an applied voltage of 1.5 V in an ice bath (below 5 °C) on a (a) bare WO $_3$ /BiVO $_4$  and (b) WO $_3$ /BiVO $_4$ /Al $_2$ O $_3$  photoanodes.

generation via the two-electron oxidation of H2O.28 Even in the case of using the WO<sub>3</sub>/BiVO<sub>4</sub>/Al<sub>2</sub>O<sub>3</sub> photoanode, the selectivity  $(\eta(H_2O_2))$  for  $H_2O_2$  generation was significantly enhanced with increasing concentration of KHCO<sub>3</sub>, and the  $\eta(H_2O_2)$  in the 2.0 M KHCO<sub>3</sub> agueous solution reached ca. 80% at 0.9C, whereas that using the bare WO<sub>3</sub>/BiVO<sub>4</sub> photoanode was ca. 54%. It should be noted that the selectivity  $(\eta(H_2O_2) = ca. 53\%)$ on the WO<sub>3</sub>/BiVO<sub>4</sub>/Al<sub>2</sub>O<sub>3</sub> photoanode in lowly concentrated KHCO<sub>3</sub> (0.1 M) was comparable to that (ca. 54%) on the bare WO<sub>3</sub>/BiVO<sub>4</sub> photoanode in highly concentrated KHCO<sub>3</sub> (2.0 M). This suggests that the Al<sub>2</sub>O<sub>3</sub> could effectively be contributing to oxidative H2O2 generation from H2O even in the lowly concentrated KHCO<sub>3</sub>. Moreover, as shown in Fig. 4(B), the excellent H<sub>2</sub>O<sub>2</sub> generation property on the WO<sub>3</sub>/BiVO<sub>4</sub>/Al<sub>2</sub>O<sub>3</sub> photoanode compared to the WO<sub>3</sub>/BiVO<sub>4</sub> photoanode was significantly maintained even at high electric charge up to 50C. As a result, the accumulation amount, using the WO<sub>3</sub>/BiVO<sub>4</sub>/Al<sub>2</sub>O<sub>3</sub> photoanode, reached >2500 μM at 50C, while that using the bare WO<sub>3</sub>/ BiVO<sub>4</sub> photoanode was >1300  $\mu$ M at 50C. The dependency of the applied voltage on the oxidative H2O2 generation was investigated to confirm the effect of the Al<sub>2</sub>O<sub>3</sub> coating in detail (Fig. S8; ESI†). A small change in H<sub>2</sub>O<sub>2</sub> generation performance was observed in all ranges of applied voltages (0.8-1.8 V), suggesting that the enhanced effect of introducing an Al2O3 layer is independent of the voltages applied between a photoanode as the working electrode and a Pt mesh as counter electrode using the aqueous electrolyte of the KHCO<sub>3</sub>.

Although little development with regards to highly selective H<sub>2</sub>O<sub>2</sub> generation via two-photon oxidation of H<sub>2</sub>O and accumulation using photoanodes has been reported, our method of Al<sub>2</sub>O<sub>3</sub> coating on the WO<sub>3</sub>/BiVO<sub>4</sub> photoanode produced tremendous improvement in selective H2O2 generation and accumulation from H<sub>2</sub>O in a KHCO<sub>3</sub> aqueous electrolyte. It is speculated that the specific enhancement of selectivity for H2O2 generation on the WO<sub>3</sub>/BiVO<sub>4</sub>/Al<sub>2</sub>O<sub>3</sub> photoanode may be caused by a blocking effect, on the mesoporous Al<sub>2</sub>O<sub>3</sub> layer, that inhibits oxidative H<sub>2</sub>O<sub>2</sub> degradation into O<sub>2</sub> on the BiVO<sub>4</sub>. To investigate the blocking effect on the Al<sub>2</sub>O<sub>3</sub> layer, a degradation property test of H<sub>2</sub>O<sub>2</sub> was performed in a 2.0 M KHCO<sub>3</sub> aqueous solution containing  $H_2O_2$  (550  $\mu$ M) in the presence of the bare WO<sub>3</sub>/BiVO<sub>4</sub> or WO<sub>3</sub>/BiVO<sub>4</sub>/Al<sub>2</sub>O<sub>3</sub> photoanodes in presence or absence of simulated solar light irradiation in an ice bath (below 5 °C). In both cases, as shown in Fig. 5, almost all the initial amount of H<sub>2</sub>O<sub>2</sub> was maintained in the dark condition, however, the H2O2 amount drastically decreased with irradiation by simulated solar light, suggesting that the H<sub>2</sub>O<sub>2</sub> was decomposed by photocarriers (excited electrons and holes) produced on the BiVO<sub>4</sub>. It should be noted that the H<sub>2</sub>O<sub>2</sub> degradation in the presence of the WO<sub>3</sub>/BiVO<sub>4</sub>/Al<sub>2</sub>O<sub>3</sub> photoanode was dramatically inhibited compared to the degradation in the presence of a bare WO<sub>3</sub>/BiVO<sub>4</sub> photoanode. The oxidative H<sub>2</sub>O<sub>2</sub> generation test was also confirmed in a 2.0 M KHCO<sub>3</sub> aqueous electrolyte, initially containing  $H_2O_2$  (210  $\mu$ M) on the bare WO<sub>3</sub>/BiVO<sub>4</sub> and WO<sub>3</sub>/BiVO<sub>4</sub>/Al<sub>2</sub>O<sub>3</sub> photoanodes, to track the generated H<sub>2</sub>O<sub>2</sub> degradation behaviour in more detail (Fig. 6). The generated rates of H<sub>2</sub>O<sub>2</sub> were reduced by the initial addition of H<sub>2</sub>O<sub>2</sub> in both cases of presence or absence of Al<sub>2</sub>O<sub>3</sub>.

**RSC Advances** Paper

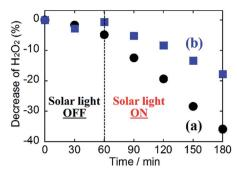


Fig. 5 Degradation properties of  $H_2O_2$  (550  $\mu M$ ) initially added in a 2.0 M KHCO<sub>3</sub> aqueous solution in an ice bath (below 5 °C) under CO<sub>2</sub> bubbling and simulated solar light irradiation in the presence of a (a) WO<sub>3</sub>/BiVO<sub>4</sub> and (b) WO<sub>3</sub>/BiVO<sub>4</sub>/Al<sub>2</sub>O<sub>3</sub> photoanodes at no applied

However, the decreasing rate of H<sub>2</sub>O<sub>2</sub> generation was significantly inhibited, from ca. 61% to ca. 39%, by introducing the Al<sub>2</sub>O<sub>3</sub> layer on the WO<sub>3</sub>/BiVO<sub>4</sub> photoanode. These results suggest that introducing the Al<sub>2</sub>O<sub>3</sub> layer significantly contributed to the highly selective H<sub>2</sub>O<sub>2</sub> generation and accumulation from H<sub>2</sub>O, with a high photocurrent property, by a blocking effect that inhibited the oxidative degradation of generated H<sub>2</sub>O<sub>2</sub>. The mechanism of blocking effect is proposed that the H<sub>2</sub>O<sub>2</sub> generated on the BiVO<sub>4</sub> in the WO<sub>3</sub>/BiVO<sub>4</sub>/Al<sub>2</sub>O<sub>3</sub> photoanode diffuses in electrolyte of KHCO3 aqueous solution through mesoporous of the Al<sub>2</sub>O<sub>3</sub>, and contact of the H<sub>2</sub>O<sub>2</sub> diffused in electrolyte with the BiVO4 covered uniformly and smoothly Al<sub>2</sub>O<sub>3</sub> may be significantly inhibited compared with that with bare BiVO<sub>4</sub>, resulting in the formation of effective inhibition of oxidative H<sub>2</sub>O<sub>2</sub> degradation. Furthermore, there may be other possible mechanisms such as a blocking effect of a direct O<sub>2</sub> evolution site via a 4-photon process covering by Al<sub>2</sub>O<sub>3</sub>, or an enrichment effect resulting from the increasing KHCO<sub>3</sub> concentration around the photoanode based on the acid-base adsorption between HCO3- (a weak base) and the weakly acidic sites on the Al<sub>2</sub>O<sub>3</sub> surface, related to the good

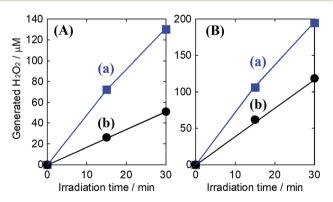


Fig. 6 Comparison of oxidative H<sub>2</sub>O<sub>2</sub> generation in a 2.0 M KHCO<sub>3</sub> aqueous electrolyte (a) in the absence of or (b) containing initiallyadded  $H_2O_2$  (210  $\mu$ M) in an ice bath (below 5 °C) on a (A)  $WO_3/BiVO_4$ and (B) WO<sub>3</sub>/BiVO<sub>4</sub>/Al<sub>2</sub>O<sub>3</sub> photoanodes under simulated solar light irradiation at steady photocurrent of 1 mA.

 $\eta(H_2O_2)$  in lower KHCO<sub>3</sub> concentration, as shown in Fig. 4(A). The tracking and contribution of these other mechanisms, on the Al<sub>2</sub>O<sub>3</sub> layer, is currently under investigation.

#### Conclusions

In summary, various metal oxides were coated onto a WO<sub>3</sub>/ BiVO<sub>4</sub> photoanode to enhance the selectivity (faradaic efficiency) of oxidative H<sub>2</sub>O<sub>2</sub> generation, in an aqueous electrolyte of KHCO3, from water under solar light irradiation. Among the various metal oxides, the Al<sub>2</sub>O<sub>3</sub> coating, which produced a mesoporous and amorphous structure on the WO<sub>3</sub>/BiVO<sub>4</sub> photoanode, achieved excellent oxidative H2O2 generation at a selectivity of ca. 80% and an accumulation of >2500  $\mu$ M (50C). Interestingly, the Al<sub>2</sub>O<sub>3</sub>-coated WO<sub>3</sub>/BiVO<sub>4</sub> photoanode dramatically inhibited oxidative degradation of H<sub>2</sub>O<sub>2</sub> generated on the WO<sub>3</sub>/BiVO<sub>4</sub> photoanode after introducing the Al<sub>2</sub>O<sub>3</sub> layer. This study contributes to developing a promising design for a clean H<sub>2</sub>O<sub>2</sub> production system that uses only water as the raw material under solar light irradiation. More effective dreamy H2O2 generation, at an excellent selectivity close to 100%, can be expected by modifying the surface-treatment technology, and it is currently under investigation.

### Conflicts of interest

There are no conflicts to declare.

## Acknowledgements

The present work was partially supported by JSPS KAKENHI Grant Number 26810105 and the International Joint Research Program for Innovative Energy Technology. We thank Dr Etsuko Fujita (Brookhaven National Laboratory) discussions.

### Notes and references

- 1 A. Fujishima and K. Honda, Nature, 1972, 238, 37.
- 2 Z. G. Zou, J. H. Ye, K. Sayama and H. Arakawa, Nature, 2001, 414, 625.
- 3 A. Kudo and Y. Miseki, Chem. Soc. Rev., 2009, 38, 253.
- 4 K. Maeda, K. Teramura, D. Lu, T. Takata, N. Saito, Y. Inoue and K. Domen, Nature, 2006, 440, 295.
- 5 K. Fuku, K. Hashimoto and H. Kominami, Chem. Commun., 2010, 46, 5118.
- 6 K. Fuku, T. Kamegawa, K. Mori and H. Yamashita, Chem.-Asian J., 2012, 7, 1366.
- 7 K. Fuku, R. Hayashi, S. Takakura, T. Kamegawa, K. Mori and H. Yamashita, Angew. Chem., Int. Ed., 2013, 52, 7446.
- 8 B. D. Alexander, P. J. Kulesza, I. Rutkowska, R. Solarska and J. Augustynski, J. Mater. Chem., 2008, 18, 2298.
- 9 K. Sayama, A. Nomura, Z. Zou, R. Abe, Y. Abe and H. Arakawa, Chem. Commun., 2003, 2908.
- 10 P. Chatchai, Y. Murakami, S. Kishioka, A. Y. Nosaka and Y. Nosaka, Electrochim. Acta, 2009, 54, 1147.

Paper

11 R. Saito, Y. Miseki and K. Sayama, *Chem. Commun.*, 2012, **48**, 3833.

- 12 I. Fujimoto, N. Wang, R. Saito, Y. Miseki, T. Gunji and K. Sayama, *Int. J. Hydrogen Energy*, 2014, **39**, 2454.
- 13 X. Shi, I. Y. Choi, K. Zhang, J. Kwon, D. Y. Kim, J. K. Lee, S. H. Oh, J. K. Kim and J. H. Park, *Nat. Commun.*, 2014, 5, 4775.
- 14 T. W. Kim and K. S. Choi, Science, 2014, 343, 990.
- 15 Y. Liu, Y. Guo, L. T. Schelhas, M. Li and J. W. Ager III, *J. Phys. Chem. C*, 2016, **120**, 23449.
- 16 L. H. Hess, J. K. Cooper, A. Loiudice, C. M. Jiang, R. Buonsanti and I. D. Sharp, *Nano Energy*, 2017, 34, 375.
- 17 J. Su, L. Guo, N. Bao and C. A. Grimes, Nano Lett., 2011, 11, 1928.
- 18 P. M. Rao, L. Cai, C. Liu, I. S. Cho, C. H. Lee, J. M. Weisse, P. Yang and X. Zheng, *Nano Lett.*, 2014, 14, 1099.
- 19 I. Grigioni, K. G. Stamplecoskie, D. H. Jara, M. V. Dozzi, A. Oriana, G. Cerullo, P. V. Kamat and E. Selli, ACS Energy Lett., 2017, 2, 1362.
- 20 K. Mase, M. Yoneda, Y. Yamada and S. Fukuzumi, ACS Energy Lett., 2016, 1, 913.
- 21 F. M. Toma, J. K. Cooper, V. Kunzelmann, M. T. McDowell, J. Yu, D. M. Larson, N. J. Borys, C. Abelyan, J. W. Beeman,

- K. M. Yu, J. Yang, L. Chen, M. R. Shaner, J. Spurgeon, F. A. Houle, K. A. Persson and I. D. Sharp, *Nat. Commun.*, 2016, 7, 12012.
- 22 J. Y. Kim, G. Magesh, D. H. Youn, J. W. Jang, J. Kubota, K. Domen and J. S. Lee, *Sci. Rep.*, 2013, 3, 2681.
- 23 Q. Mi, A. Zhanaidarova, B. S. Brunschwig, H. B. Gray and N. S. Lewis, *Energy Environ. Sci.*, 2012, 5, 5694.
- 24 J. C. Hill and K. S. Choi, J. Phys. Chem. C, 2012, 116, 7612.
- 25 K. Ueno and H. Misawa, NPG Asia Mater., 2013, 5, e61.
- 26 K. Fuku, N. Wang, Y. Miseki, T. Funaki and K. Sayama, ChemSusChem, 2015, 8, 1593.
- 27 H. G. Cha and K. S. Choi, Nat. Chem., 2015, 7, 328.
- 28 K. Fuku and K. Sayama, Chem. Commun., 2016, 52, 5406.
- 29 K. Fuku, Y. Miyase, Y. Miseki, T. Funaki, T. Gunji and K. Sayama, *Chem.-Asian J.*, 2017, **12**, 1111.
- 30 K. Fuku, Y. Miyase, Y. Miseki, T. Gunji and K. Sayama, *ChemistrySelect*, 2016, 1, 5721.
- 31 T. Shiragami, H. Nakamura, J. Matsumoto, M. Yasuda, Y. Suzuri, H. Tachibana and H. Inoue, *J. Photochem. Photobiol.*, A, 2015, 313, 131.
- 32 R. Saito, Y. Miseki, W. Nini and K. Sayama, *ACS Comb. Sci.*, 2015, 17, 592.